

Enhancement of switching speed of BiFeO₃ capacitors by magnetic fields

E. J. Guo, S. Das, and A. Herklotz

Citation: [APL Materials](#) **2**, 096107 (2014); doi: 10.1063/1.4894758

View online: <https://doi.org/10.1063/1.4894758>

View Table of Contents: <http://aip.scitation.org/toc/apm/2/9>

Published by the [American Institute of Physics](#)

Articles you may be interested in

[Tuning the switching time of BiFeO₃ capacitors by electrodes' conductivity](#)

Applied Physics Letters **103**, 022905 (2013); 10.1063/1.4813419

[Ferroelectric or non-ferroelectric: Why so many materials exhibit “ferroelectricity” on the nanoscale](#)

Applied Physics Reviews **4**, 021302 (2017); 10.1063/1.4979015

[Tetragonal BiFeO₃ on yttria-stabilized zirconia](#)

APL Materials **3**, 116104 (2015); 10.1063/1.4935310

[Electric field control of magnetism using BiFeO₃-based heterostructures](#)

Applied Physics Reviews **1**, 021303 (2014); 10.1063/1.4870957

[Strain controlled ferroelectric switching time of BiFeO₃ capacitors](#)

Applied Physics Letters **101**, 242908 (2012); 10.1063/1.4772006

[Bulk photovoltaic effect in monodomain BiFeO₃ thin films](#)

Applied Physics Letters **110**, 183902 (2017); 10.1063/1.4983032

PHYSICS TODAY

WHITEPAPERS

ADVANCED LIGHT CURE ADHESIVES

Take a closer look at what these environmentally friendly adhesive systems can do

READ NOW

PRESENTED BY
 **MASTERBOND**
ADHESIVES | SEALANTS | COATINGS

Enhancement of switching speed of BiFeO₃ capacitors by magnetic fields

E. J. Guo,^{1,2,a} S. Das,^{1,2} and A. Herklotz^{1,2,b}

¹*Institute for Physics, Martin-Luther-University Halle-Wittenberg, 06120 Halle, Germany*

²*Institute for Metallic Materials, IFW Dresden, Postfach 270116, 01171 Dresden, Germany*

(Received 9 June 2014; accepted 25 August 2014; published online 5 September 2014)

The effect of a magnetic field on the ferroelectric switching kinetics of BiFeO₃ (BFO) capacitors with La_{0.8}Ca_{0.2}MnO₃ (LCMO) bottom electrode and Pt top contact has been investigated. We find a strong dependence of the remnant polarization and coercive field on the magnetic field. The switching time can be systematically tuned by magnetic field and reaches a tenfold reduction around the Curie temperature of LCMO at 4 T. We attribute this behavior to the splitting of the voltage drops across the BFO film and the LCMO bottom electrode, which can be strongly influenced by an external magnetic field due to the magnetoresistance. Further experiments on the BFO capacitors with SrRuO₃ bottom electrodes show little magnetic field dependence of ferroelectric switching confirming our interpretation. Our results provide an efficient route to control the ferroelectric switching speed through the magnetic field, implying potential application in multifunctional devices. © 2014 Author(s). All article content, except where otherwise noted, is licensed under a Creative Commons Attribution 3.0 Unported License. [<http://dx.doi.org/10.1063/1.4894758>]

Tuning of magnetism by an electric field or the ferroelectricity by a magnetic field in the multiferroic materials has been attractive for both device application and fundamental physics. Among the few discovered single-phase multiferroic materials, BiFeO₃ (BFO) exhibits both ferroelectricity as well as antiferromagnetism at room temperature.^{1–5} It has been established that the antiferromagnetic domain structures in BFO films are coupled with ferroelectric domains allowing one to achieve electric control on magnetic properties and vice versa.^{4,5} However, the weak magnetoelectric coupling parameter of BFO may limit its wide applications. To overcome this intrinsic limit of single-phased multiferroic materials, artificially designed two-phase systems consisting of separated magnetic and ferroelectric materials serve as an alternative approach and has been widely studied in recent years.^{6–10} Among several candidate materials, the doped manganites, such as La_{1-x}Sr_xMnO₃ and La_{1-x}Ca_xMnO₃, are intensively used either as functional layer or as electrode due to the similar perovskite structure and low lattice mismatch to the BFO layer, as well as good conductivity.^{8–10} Over the years, some interesting properties are observed at their interfaces. For instance, a novel ferromagnetic state has been found at the interface between the ferromagnetic La_{0.7}Sr_{0.3}MnO₃ layer and the antiferromagnetic BFO film.⁹ In turn, the interfacial ferromagnetic state of BFO can influence its ferroelectric properties. Very recently, Liu *et al.*¹⁰ investigated the magnetic field dependence of ferroelectric properties of Au/BFO/La_{5/8}Ca_{3/8}MnO₃ heterostructures and gave a comprehensive overview of possible physical mechanisms behind the aforementioned phenomena. Controlling ferroelectric switching speed is crucial for the development of exchange-coupled magnetoelectric devices. For many years, the influences of the bottom electrodes' conductivity on the ferroelectric switching speed were seldom addressed. In our previous work, we have shown that switching speed

^aAuthor to whom correspondence should be addressed. Present address: Institute for Physics, Johannes-Gutenberg University Mainz, 55099 Mainz, Germany. Electronic mail: ejguophysics@gmail.com

^bPresent address: Materials Science and Technology Division, Oak Ridge National Laboratory, Oak Ridge, Tennessee 37831-6056, USA.

can be tuned by modulating the conductivity of bottom electrode through elastoresistance.¹¹ An even easier and more effective way to perform such modulation is thought to be altering the magnetic field. In this paper, we explore the effects of magnetic field on the ferroelectric switching time of BFO capacitors with $\text{La}_{0.8}\text{Ca}_{0.2}\text{MnO}_3$ (LCMO) bottom electrode and Pt top contacts. A tenfold reduction of the switching time is observed close to the Curie temperature of LCMO. We argue that splitting of the applied voltage across the BFO film and LCMO electrode, which is largely influenced due to the magnetoresistance, is responsible for our results.

The 250 nm thick BFO thin films are deposited on LCMO film (~ 15 nm) covered $0.72\text{Pb}(\text{Mg}_{1/3}\text{Nb}_{2/3})\text{O}_3\text{-}0.28\text{PbTiO}_3$ (PMN-PT) (001) single crystal substrate by pulsed laser deposition. Details of deposition process can be found in Ref. 11. The piezoelectric substrate is chosen due to our previous work to investigate the ferroelectric switching dynamics under the reversible controlled strains.^{12,13} We also note that our PMN-PT substrate shows a diamagnetic behavior under applied magnetic fields. It has a relative small magnetic susceptibility due to the inevitable impurities during the crystal manufacturing process. Meanwhile, the PMN-PT single crystal shows no significant magnetostriction, thus, negligible response under applied magnetic fields can be observed. The structural analysis of our films has been done by high-resolution x-ray diffraction (XRD). The θ - 2θ XRD patterns reveal the single pseudocubic phase and high crystallinity for all layers. Circular Pt top contacts with a diameter of $100\ \mu\text{m}$ are deposited at room temperature through a shadow mask. The ferroelectric measurements are conducted through the Pt top contact and LCMO bottom electrode using a TF Analyzer 1000 at 1 kHz. The remnant polarization (P_r) and the coercive field (E_C) of the BFO capacitors at 300 K are about $65\ \mu\text{C}/\text{cm}^2$ and 265 kV/cm, respectively, as measured from the well-defined square shape-like hysteresis loop,¹¹ which are comparable with previous work.²⁻⁵ Further local measurements on the piezoresponse force microscopy (PFM) also confirm the good ferroelectric properties of our BFO films.¹¹ The ferroelectric switching measurements at low temperature under the magnetic field are carried out by Magnetic Property Measurement System (MPMS-5T, Quantum Design). The magnetic field was applied parallel to the film surface (ab -plane).

The ferroelectric hysteresis loops of BFO capacitors measured at different magnetic fields and temperatures are shown in Figs. 1(a)–1(c). In our previous work,¹¹ we had shown E_C increases with decreasing temperature towards a maximum at ~ 200 K under zero magnetic field, while, P_r decreases from $65\ \mu\text{C}/\text{cm}^2$ at the room temperature to $48.5\ \mu\text{C}/\text{cm}^2$ at 50 K. The strong temperature dependence of P_r is most likely related to the reduction of leakage currents during the switching measurements. The hysteresis loop is not completely closed at the room temperature and becomes more saturated at low temperatures. The ferroelectric hysteresis loops show strong magnetic field dependence and are tuned systematically by the applied fields. Figs. 1(d) and 1(f) show the relative changes of $\Delta P_r(H) = [P_r(H) - P_r(0)] \times 100\% / P_r(0)$ and $\Delta E_C(H) = [E_C(H) - E_C(0)] \times 100\% / E_C(0)$ as a function of magnetic fields at temperatures of 10, 100, 150, 200, 250, and 300 K, respectively. For $T > 150$ K, P_r increases with applied fields in contrast to $T < 150$ K, where P_r decreases. E_C always decreases with the magnetic fields at all temperatures. In order to have a better illustration, the temperature dependences of $\Delta P_r(H)$ and $\Delta E_C(H)$ measured at 4 T are shown in Figs. 1(e) and 1(g), respectively. The $\Delta P_r|_{H=4\text{T}}$ increases with decreasing temperature towards a maximum of $\sim 6\%$ at 200 K, followed by a rapid decrease to a negative value of about -0.5% at 10 K. The $\Delta E_C|_{H=4\text{T}}$ shows an opposite behavior. A negative peak of $\sim -50\%$ was found at 200 K. The magnetic field and temperature dependences of ferroelectric switching parameters (P_r and E_C) resemble that of the electrical conductivity of the doped manganites. Therefore, the temperature dependence of the resistivity of the LCMO bottom electrode and its magnetic response are carefully measured via the standard four-probe method. At zero magnetic fields, the resistance of LCMO increases as the temperature decreases and undergoes a sharp drop at ~ 200 K, demonstrating an insulator-to-metal (I - M) transition. With the increase of the magnetic field, the resistance decreases dramatically over a broad range of temperature. Fig. 2(a) shows the magnetic field dependence of the magnetoresistance $\text{MR} = [R(H) - R(0)] \times 100\% / R(0)$ of the LCMO bottom electrode measured at various temperatures. It shows a typical variation observed in many doped manganite thin films.¹⁴⁻¹⁶ Interestingly, the MR curves shows a maximum value of -73% at 200 K that coincides with the minimum of $\Delta E_C|_{H=4\text{T}}$ [Fig. 2(b)]. Also, the similarity of the magnetic field dependence of $\Delta E_C(H)$ and $\text{MR}(H)$ indicates that the ferroelectric switching of the BFO capacitor is related to the resistance of bottom electrode.

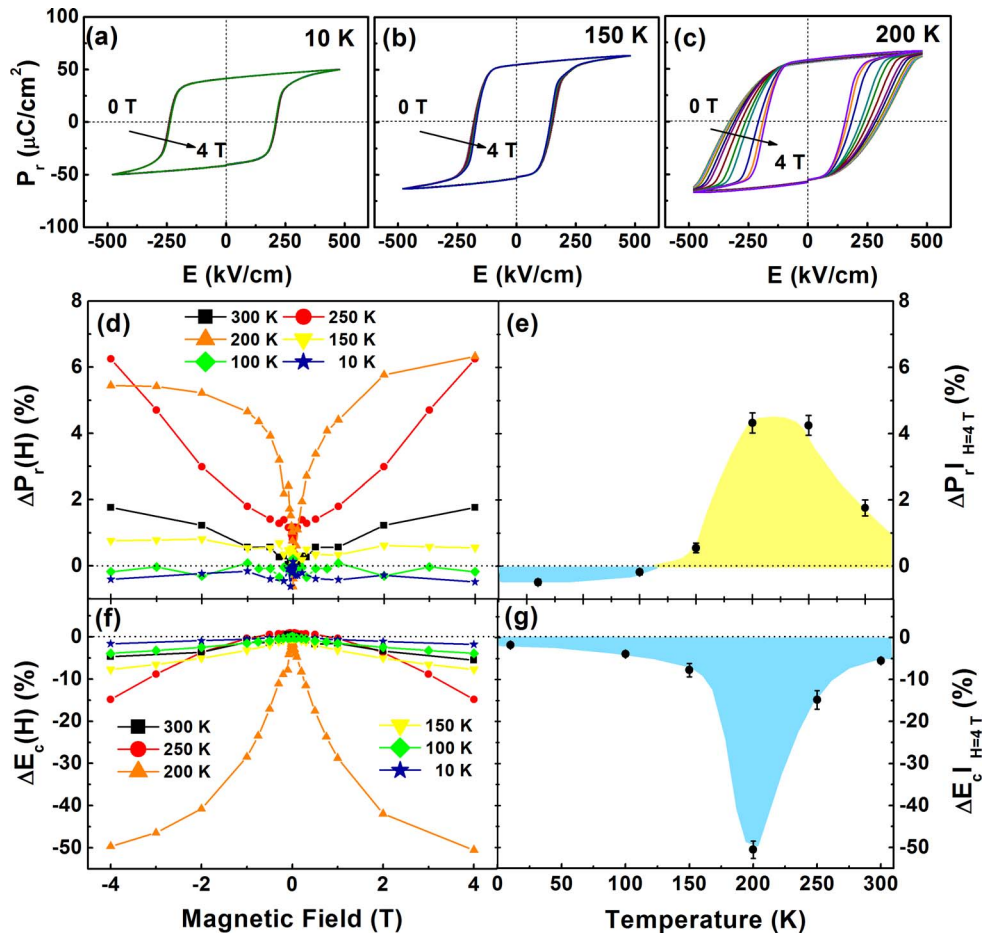


FIG. 1. (a)-(c) The ferroelectric hysteresis loops of a Pt/BFO/LCMO capacitor at different magnetic fields measured at 10, 150, 200 K, respectively. The magnetic field dependence of relative changes in (d) P_r and (f) E_c are measured at 10, 100, 150, 200, 250, and 300 K, respectively. (e) and (g) The temperature dependence of ΔP_r and ΔE_c under 4 T, respectively.

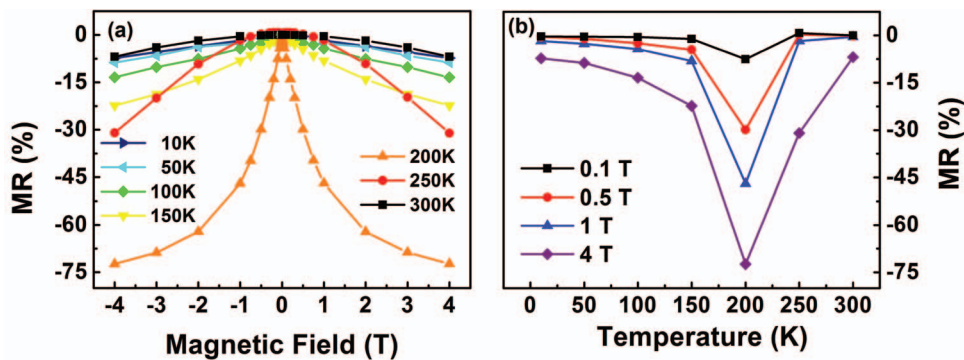


FIG. 2. (a) Magnetic field dependence of the magnetoresistance $\text{MR} = [R(H) - R(0)] \times 100\% / R(0)$ of LCMO bottom electrode measured at various temperatures. (b) Temperature dependence of the MR under magnetic fields of 0.1, 0.5, 1, and 4 T.

Earlier pointed out that the resistance of the bottom electrode cannot be ignored anymore when the impedance of ferroelectric film is comparable with it.¹¹ The impedance of the capacitor is decreasing dramatically with increasing the measuring frequency. In our case, considering the geometry of the capacitor and the measured P_r and E_c , the estimated value of the impedance of BFO film $Z_{\text{BFO}} = 1/f \cdot (E_c/4\pi P_r) \cdot d/A$ varies from 26 k Ω to 26 Ω when the measuring frequency

(*f*) increased from 1 kHz to 1 MHz, where d is the film thickness and A is the switching area of BFO capacitor. The measured resistance of bottom electrode is 18.3 k Ω under zero magnetic field at 300 K, which is in the same order of magnitude as the impedance of the BFO film even at 1 kHz. Hence, the electric voltage will split between the BFO film and the LCMO bottom electrode. At low switching speed, i.e., measured at a lower electric field, it may be still safe to ignore the influence of the bottom electrode due to the high impedance of the BFO film. However, when the switching speed becomes faster, i.e., measured at a larger electric field, the problem will become more severe as the majority of the voltages will drop at the bottom electrode. The changes of the bottom electrodes' resistance will greatly influence the ferroelectric switching measurements.

According to the above statement, the magnetic field dependence of E_C and P_r can be understood as follows. Our measured E_C of capacitor is the sum of two contributions, one is the real (E_C)_{real} of the BFO film and the other one is from the electric field at the LCMO electrode:

$$E_C = (E_C)_{\text{real}} + V_{\text{LCMO}}/d, \quad (1)$$

where, the V_{LCMO} is the voltage across the LCMO which can be changed with external magnetic fields and temperatures. Under the same magnetic fields, as the temperature decreases from room temperature to the I - M transition temperature, the magnetoresistance of LCMO increases dramatically and reaches a maximum value. Therefore, the negative peak in the $\Delta E_C|_{H=4T}$ - T curve can be attributed to the huge reduction of the bottom electrodes' resistance induced by magnetic field. With the temperature further decreasing, the magnetoresistance becomes smaller and the real nature of the enhancement of coercive field comes out resulting in the increment of $\Delta E_C|_{H=4T}$. The polarization P is calculated through integrating the switching currents I over pulse time t ,

$$P = \left(\int_{t_1}^{t_2} I dt / A \right) - \varepsilon_0 E, \quad (2)$$

$$I = \frac{V}{Z_{\text{BFO}} + R_{\text{LCMO}}}, \quad (3)$$

where, ε_0 is the value of absolute dielectric permittivity in vacuum, V is the applied voltage, and R_{LCMO} is the bottom electrode's resistance. As the magnetic fields increasing, the bottom electrodes' resistance decreases resulting in the enhancement of switching currents. The increase of the P_r under the magnetic fields at a fixed temperature can be understood in this term. However, compared with $\Delta E_C|_{H=4T} \sim -50\%$, the maximum change of $\Delta P_r|_{H=4T}$ is only 6%. Here, we have to point out that the influence of magnetic fields on the polarization is also strongly related to the magnetoelectric coupling at the interfaces between the electrodes and ferroelectric layers. The double exchange interaction between the Fe and Mn may exist at the interface between the BFO and LCMO layer. Thus, a modification of surface electronic state could enhance the conductivity, resulting in a faster switching speed. Moreover, early works also argued that the magnetostriction effect in the manganite films and also the depolarization fields may contribute to the magnetic field dependencies of ferroelectric parameters.¹⁰ Clearly, magnetic field induced effects are still not fully understood so far and need to be further investigated.

Following the above consideration, the magnetoresistance may also influence the ferroelectric switching speed of BFO capacitors. Therefore, pulse measurements based on the positive-up-negative-down (PUND) method are conducted in order to investigate the domain kinetics of BFO capacitors. Here, the switched polarization $\Delta P(t)$ can be obtained by varying the pulse time t at given electric fields E . According to the Kolmogorov-Avrami-Ishibashi (KAI) model, $\Delta P(t)$ can be written as^{17,18}

$$\Delta P(t) = 2P_s \{1 - \exp[-(t/t_{\text{sw}})^n]\}, \quad (4)$$

where P_s is the spontaneous polarization, t_{sw} is a characteristic switching time for domain growth, and n is the effective growth dimension. Figs. 3(a) and 3(b) show the normalized switched polarization $\Delta P(t)/2P_s$ for $E = 440$ and 100 kV/cm under various magnetic fields at 200 K, respectively. Our measured data (scatters) agree well with the KAI model fittings (solid lines) based on Eq. (4), indicating the good quality of the BFO films. Obviously, the magnetic field leads to a huge

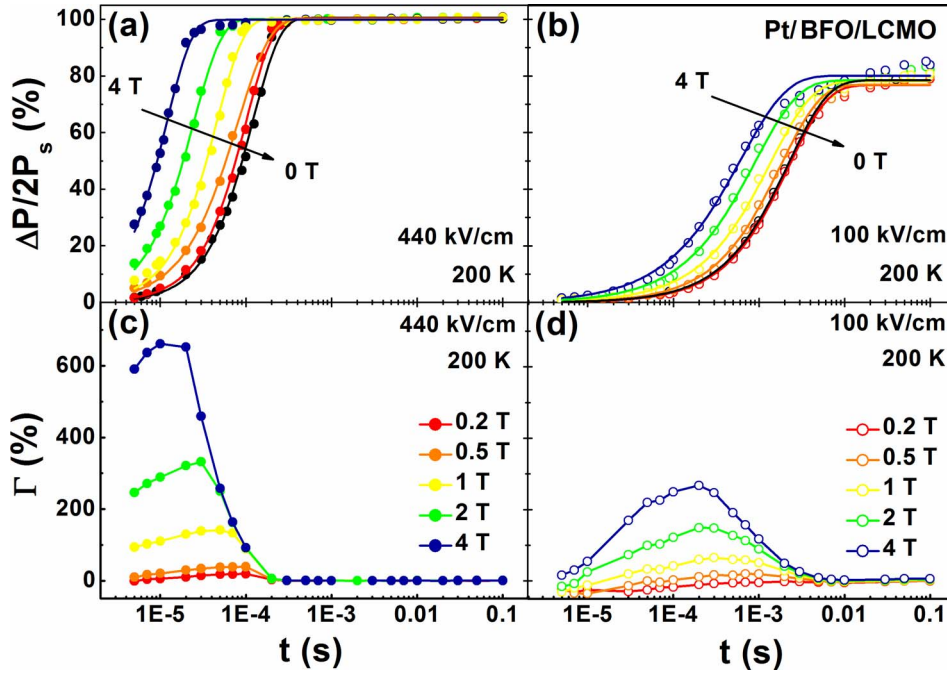


FIG. 3. Switched polarization ($\Delta P/2P_s$) vs pulse time (t) for driving forces of (a) 440 kV/cm and (b) 100 kV/cm under various magnetic fields at 200 K. Pulse time dependence of the relative changes $\Gamma = [\Delta P(t, H) - \Delta P(t, 0)] \times 100\% / \Delta P(t, 0)$ between various magnetic fields and zero magnetic field for driving forces of (c) 440 kV/cm and (d) 100 kV/cm measured at 200 K, respectively.

enhancement of $\Delta P(t)$. In order to get a better illustration, the relative change $\Gamma = [\Delta P(t, H) - \Delta P(t, 0)] \times 100\% / \Delta P(t, 0)$ is calculated for $E = 440$ and 100 kV/cm, as shown in Figs. 3(c) and 3(d), respectively. The maximum Γ increases dramatically with increasing magnetic field and reaches 660% and 265% for $E = 440$ and 100 kV/cm at 4 T, respectively. This relative change is one order of magnitude higher than that induced by the elastoresistance of the bottom electrode as reported in earlier.¹³

Usually, in a large-area capacitor, the domain wall velocity is approximately proportional to $1/t_{sw}$ because a huge number of nucleation sites exist simultaneously and the nucleation process happens in a short time.¹⁹ Therefore, $1/t_{sw}$ is assumed to reflect the speed of the domain wall motion. The switching time t_{sw} is calculated according to Eq. (4) and the $1/t_{sw}$ vs E curves at various magnetic fields are plotted in Fig. 4(a). At zero magnetic field, the domain wall velocity increases with a higher electric field, as has been found earlier in our work (Ref. 11). With increasing the magnetic field, the domain wall motions become faster with electric fields. Fig. 4(b) shows the relative change of switching time $\Delta t_{sw} = [t_{sw}(H) - t_{sw}(0)] \times 100\% / t_{sw}(0)$ vs E at different magnetic fields. Notably, as $E < 150$ kV/cm, Δt_{sw} tends to zero indicating accelerating speed reduces at lower electric fields. For $E > 150$ kV/cm, Δt_{sw} reaches a saturated value with a minimum of -90% at 4 T. The ferroelectric switching time is strongly dependent on the temperature, as shown in Fig. 5(a), $1/t_{sw}$ decreases monotonically with increasing temperature. The relative change Δt_{sw} shows a negative peak of -90% for at $T \sim 200$ K [Fig. 5(b)]. This coincides with the temperature dependence of the MR of the LCMO bottom electrode [Fig. 2(b)]. Therefore, the impact of MR on the $\Delta P(t)$ and t_{sw} can be explained as follows. At larger electric fields, regarding to the higher switching frequency, Z_{BFO} will be a smaller value as discussed above. The voltage at the bottom electrode will be reduced due to the large MR, leading to an enhancement of the voltage at the BFO films. A larger switched polarization and a faster acceleration of domain wall motion under higher electric fields are understandable. On the contrary, at lower electric fields, Z_{BFO} is a large value. Although the MR is the same, its effects on the voltage at the BFO film will become weaker, resulting in a relative smaller effects on the $\Delta P(t)$ and t_{sw} . Moreover, compared to the elastoresistance effect of the bottom electrode on the maximum

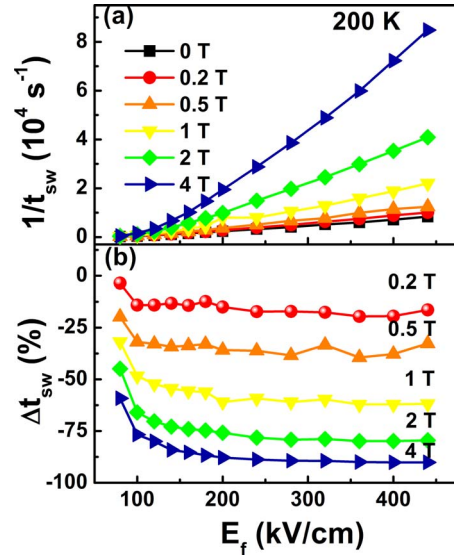


FIG. 4. The electric field dependence of (a) $1/t_{sw}$ and (b) $\Delta t_{sw} = [t_{sw}(H) - t_{sw}(0)] \times 100\% / t_{sw}(0)$ under magnetic fields of 0, 0.2, 0.5, 1, 2, and 4 T, respectively, at 200 K.

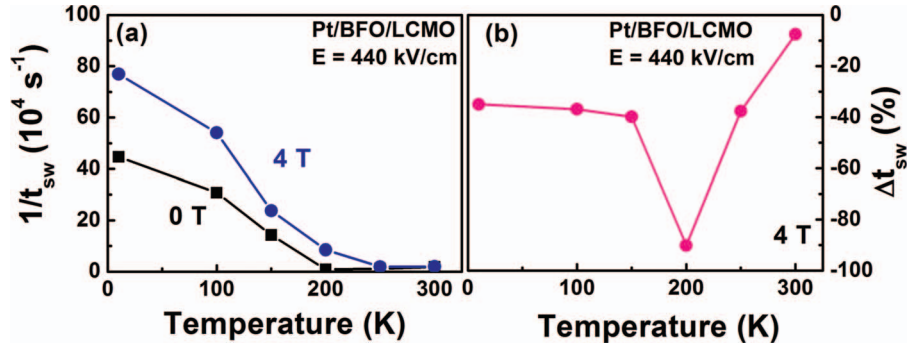


FIG. 5. (a) Temperature dependence of $1/t_{sw}$ for the driving force of 440 kV/cm under 0 and 4 T. (b) Temperature dependence of Δt_{sw} between 0 and 4 T.

changes of $\Delta P(t)$ ($\sim 85\%$) and t_{sw} ($\sim -40\%$), the magnetoresistance effect induced larger changes of $\Delta P(t)$ ($\sim 660\%$) and t_{sw} ($\sim -90\%$), respectively, which can be attributed to the larger MR up to -73% at 4 T. Here, we predict that larger effects on the polarization and switching speed can be achieved with lower magnetic fields by using more magnetic-sensitive electrode materials, such as cobaltates (like $\text{La}_{1-x}\text{Sr}_x\text{CoO}_3$) or nickelates (LaNiO_3).

Finally, in order to confirm our interpretation, similar experiments were carried out on BFO capacitors grown on PMN-PT substrates with SrRuO_3 (SRO) bottom electrode and Pt top contacts. The deposition process and structural analysis can be found in our previous work.¹³ The thicknesses of both BFO films are approximately in the same range of ~ 250 nm. As shown in the inset of Fig. 6(a), well defined square-shape-like hysteresis loops were obtained. The hysteresis loops are nearly unchanged when the magnetic field increases from 0 to 4 T. The P_r and E_C are around $67 \mu\text{C}/\text{cm}^2$ and 238 kV/cm, respectively, and show very small magnetic field dependences. At room temperature and zero magnetic fields, $1/t_{sw}$ of the BFO capacitor with SRO bottom electrode shows a higher value than that of the BFO capacitor with LCMO bottom electrode [Fig. 6(b)]. Although it is difficult to compare these two kinds of BFO capacitors due to their differences in the defect level and interface conditions, R_{SRO} ($\sim 300 \Omega$) is much lower than R_{LCMO} ($\sim 18.3 \text{ k}\Omega$) resulting in a higher voltage at the BFO films under the same electric fields. Thus, a faster domain switching speed

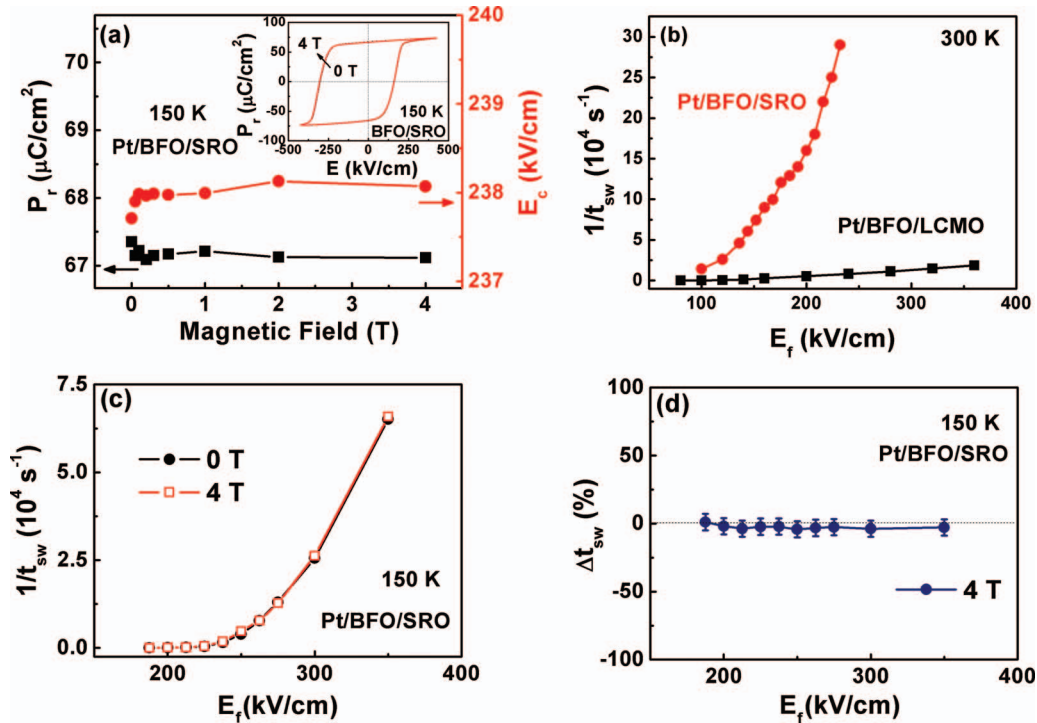


FIG. 6. (a) Magnetic field dependence of P_r and E_c of a Pt/BFO/SRO capacitor at 150 K. The inset shows the ferroelectric hysteresis loops under magnetic fields up to 4 T at measuring frequency of 1 kHz and 150 K. (b) The field dependence of $1/t_{sw}$ for Pt/BFO/SRO and Pt/BFO/LCMO capacitor measured at room temperature. The field dependence of (c) $1/t_{sw}$ and (d) Δt_{sw} between 0 and 4 T at 150 K.

on the Pt/BFO/SRO capacitor is quantitatively understandable. Fig. 6(c) shows $1/t_{sw}$ vs E curves of Pt/BFO/SRO capacitor measured under 0 and 4 T at 150 K. The difference between the two curves is almost within an error bar. In Fig. 6(d) we have shown the relative change Δt_{sw} between 0 and 4 T as a function of E_f . The magnetic field up to 4 T has little influence, less than -3% , on the switching time. This effect is quite small compared to what we found for the BFO capacitors with LCMO electrodes. As established by Gausepohl *et al.*,²⁰ SRO thin film exhibits a negative MR with temperature decreasing and reaches a maximum of $\sim -4\%$ for 7 T at the ferromagnetic transition temperature ~ 150 K. The MR of the SRO film is much smaller than that of the LCMO film. Thus, the change of voltage at the BFO film is comparably small leading to a negligible influence on the switching time.

Previously, we had shown that the elastoresistance of the bottom electrode affects the switching of ferroelectric BFO capacitors by *in situ* control of the strain state through the use of piezoelectric substrates. In this work, we further investigated tuning of domain kinetics of ferroelectric BFO capacitors through the magnetoresistance. Larger relative changes on polarization ($\sim 660\%$) and switching time ($\sim -90\%$) were obtained compared to our previous work, indicating a more effective route of controlling the ferroelectric switching. Apparently, it demonstrates strong potential applications in the multiferroic devices. The capacitance [$C_{FE} \sim (2P_r \cdot A)/(E_c \cdot d)$] of the BFO capacitor is estimated to be ~ 6 nF and the output impedance of the TF analyzer is 10Ω . The estimated RC constant of the circuit is ~ 60 ns. A faster internal switching speed of the capacitor will make the RC constant of external circuits to be the only limitation of the device's speed. It will greatly help to achieve ultrafast read/write speed FeRAM memories. We attributed these huge effects to the splitting of the voltage between the ferroelectric film and bottom electrode. BFO capacitors with different bottom electrodes were measured confirming our interpretation. Besides, the magnetic field effects on the magnetoelectric coupling at the ferroelectric film-electrode interfaces are still unclear yet. Although the magnetic field plays a little role on the domain switching time of BFO capacitor

with SRO bottom electrode, we did not rule out the interfacial effects on the ferroelectric domain switching. Indeed, it needs further investigations and exploits potential device applications.

This work was supported by Deutsche Forschungsgemeinschaft (DFG) under the grant of SFB 762 *Functionality of Oxide Interfaces*.

- ¹ J. Wang, A. Scholl, H. Zheng, S. B. Ogale, D. Viehland, D. G. Schlom, N. A. Spaldin, K. M. Rabe, M. Wuttig, L. Mohaddes, J. Neaton, U. Waghmare, T. Zhao, and R. Ramesh, *Science* **299**, 1719 (2003).
- ² H. W. Jang, S. H. Baek, D. Ortiz, C. M. Folkman, R. R. Das, Y. H. Chu, P. Shafer, J. X. Zhang, S. Choudhury, V. Vaithyanathan, Y. B. Chen, D. A. Felker, M. D. Biegalski, M. S. Rzchowski, X. Q. Pan, D. G. Schlom, L. Q. Chen, R. Ramesh, and C. B. Eom, *Phys. Rev. Lett.* **101**, 107602 (2008).
- ³ W. Eerenstein, N. D. Mathur, and J. F. Scott, *Nature* **442**, 759 (2006).
- ⁴ M. Fiebig, *J. Phys. D: Appl. Phys.* **38**, R123 (2005).
- ⁵ T. Zhao, A. Scholl, F. Zavaliche, K. Lee, M. Barry, A. Doran, M. P. Cruz, Y. H. Chu, C. Ederer, N. A. Spaldin, R. R. Das, D. M. Kim, S. H. Baek, C. B. Eom, and R. Ramesh, *Nat. Mater.* **5**, 823–829 (2006).
- ⁶ C. Thiele, K. Dörr, O. Bilani, J. Rödel, and L. Schultz, *Phys. Rev. B* **75**, 054408 (2007).
- ⁷ M. Pan, S. Hong, J. R. Guest, Y. Liu, and A. Petford-Long, *J. Phys. Appl. Phys.* **46**, 055001 (2013).
- ⁸ W. Eerenstein, M. Wiora, J. L. Prieto, J. F. Scott, and N. D. Mathur, *Nat. Mater.* **6**, 348 (2007).
- ⁹ P. Yu, J.-S. Lee, S. Okamoto, M. D. Rossell, M. Huijben, C.-H. Yang, Q. He, J. X. Zhang, S. Y. Yang, M. J. Lee, Q. M. Ramasse, R. Erni, Y.-H. Chu, D. A. Arena, C.-C. Kao, L. W. Martin, and R. Ramesh, *Phys. Rev. Lett.* **105**, 027201 (2010).
- ¹⁰ Y. Liu, Y. Yao, S. Dong, S. Yang, and X. Li, *Phys. Rev. B* **86**, 075113 (2012).
- ¹¹ E. J. Guo, A. Herklotz, R. Roth, M. Christl, S. Das, W. Widdra, and K. Dörr, *Appl. Phys. Lett.* **103**, 022905 (2013).
- ¹² A. Herklotz, E. J. Guo, M. D. Biegalski, H. M. Christen, L. Schultz, and K. Dörr, *New J. Phys.* **15**, 073021 (2013).
- ¹³ E. J. Guo, K. Dörr, and A. Herklotz, *Appl. Phys. Lett.* **101**, 242908 (2012).
- ¹⁴ P. Schiffer, A. Ramirez, W. Bao, and S.-W. Cheong, *Phys. Rev. Lett.* **75**, 3336 (1995).
- ¹⁵ Y. Tokura, H. Kuwahara, Y. Moritomo, Y. Tomioka, and A. Asamitsu, *Phys. Rev. Lett.* **76**, 3184 (1996).
- ¹⁶ A. Moreo, S. Yunoki, and E. Dagotto, *Science* **283**, 2034 (1999).
- ¹⁷ A. N. Kolmogorov, *Izv. Akad. Nauk SSSR, Ser. Math.* **3**, 355 (1937).
- ¹⁸ M. Avrami, *J. Chem. Phys.* **8**, 212 (1940).
- ¹⁹ J. Y. Jo, S. M. Yang, T. H. Kim, H. N. Lee, J.-G. Yoon, S. Park, Y. Jo, M. H. Jung, and T. W. Noh, *Phys. Rev. Lett.* **102**, 045701 (2009).
- ²⁰ S. C. Gausepohl, M. Lee, K. Char, R. A. Rao, and C. B. Eom, *Phys. Rev. B* **52**, 3459 (1995).